An Approach to Accurate Inversion of Convolution Transforms by FIR Filters

VAIRIS SHTRAUSS
Institute of Polymer Mechanics
University of Latvia
23 Aizkraukles Street, LV 1006 Riga
LATVIA
strauss@pmi.lv

Abstract: - Inversion of convolution transforms is considered by FIR filters for aperiodic band- and time-unlimited signals from the perspective attaining maximum accurate inverted waveforms with controllable noise amplification of the filter. The difficulties hampering to gain this goal, such as a lack of knowledge how the digital filter shall deviate from ideal one to produce waveforms as accurately as possible, complexity to choose optimal sampling rate, necessity to sacrifice the accuracy for suppressing noise, etc. are analysed. Based on learning in the input-output signal domain and controlling noise amplification by varying sampling rate, an approach is developed for designing maximum accurate filters, which are specified only by two user's relevant parameters: (i) the desired noise gain and (ii) the continuous time support. Implementation of the approach is illustrated by designing a digital differentiator for the logarithmic derivative and a digital estimator of the distribution of relaxation times. Simulation results are presented demonstrating that the approach allows constructing more accurate FIR filters with predefined noise amplification and support sizes compared with those designed by other commonly used techniques.

Key-Words: - Convolution Transform, Inversion, Deconvolution, FIR Filter, Accuracy, Noise Amplification, Design by Learning

1 Introduction

An important class of theoretical and practical tasks occurring in many branches of science and engineering is related to solving a problem mathematically leading to finding a function, which is interrelated to some other function by a convolution transform

$$x(t) = (y * k)(t) = \int_{-\infty}^{\infty} y(u)k(t-u)du = \int_{-\infty}^{\infty} y(t-u)k(u)du, \quad -\infty < t < \infty, \tag{1}$$

where symbol * denotes the convolution, $x(t)$ is some given or recorded function, $y(t)$ is some unknown function that we wish to recover, and $k(t)$ is kernel.

The mentioned above task is inversion of convolution transform [1], which is known also as *continuous-time deconvolution problem*. The significance of the task is obvious from the fact that convolution transforms are used to solve numerous problems of mathematical physics, and many of classical integral transforms, such as Laplace, Fourier-sine, Fourier-cosine, Hankel, Meier, etc. are either in the form (1) or can be put into it by change of variable.

In this study, we consider inversion of (1) for aperiodic band- and time-unlimited functions. Such functions are of typical use in physics [2], mechanics [3], material science [4], etc.

In the frequency domain, Eq. (1) takes the form

$$X(j\omega) = Y(j\omega)K(j\omega), \tag{2}$$

where capital letters are used for the Fourier transforms. Equation (2) allows obtaining function $y(t)$ by the inverse Fourier transform of

$$Y(j\omega) = X(j\omega)/K(j\omega). \tag{3}$$

The time-domain counterpart of Eq. (3) is the following convolution transform

$$y(t) = (x * h)(t) = \int_{-\infty}^{\infty} x(u)h(t-u)du = \int_{-\infty}^{\infty} x(t-u)h(u)du, \quad -\infty < t < \infty, \tag{4}$$

where $h(t)$ is the *inverse kernel*, which is not always be known. Contrary, the frequency spectrum of the inverse kernel can usually be determined as the reciprocal of the Fourier transform of the direct kernel

$$H(j\omega) = 1/K(j\omega). \tag{5}$$

In the case of absolute integrable direct kernel $k(t)$, it follows from the Riemann-Lebesgue lemma [5] that $|K(j\omega)|$ is a decreasing function

$$\lim_{|\omega|\to\infty} |K(j\omega)| = 0$$

and, consequently, $|H(j\omega)|$ is an infinitely increasing function

$$\lim_{|\omega|\to\infty} |H(j\omega)| = \infty . \quad (6)$$

Hence, inverse kernel $h(t)$ cannot be an integrable function, and often exists in the class of the generalized functions.

According to Eq. (4), inversion of transform (1) can be regarded as a filtering problem with an *ideal deconvolution* filter having impulse response $h(t)$ and frequency response $H(j\omega)$ producing output signal $y(t)$ in response to input signal $x(t)$. The ideal deconvolution filter has infinite support, and its key feature is infinitely increasing magnitude response (6), which is responsible for ill-posed nature of deconvolution.

The above filtering model establishes a theoretical basis for solving the continuous-time deconvolution problem by finite impulse response (FIR) deconvolution filters, which may be presented in the following non-causal form:

$$\hat{y}(mT) = \sum_{n=-(N-1)/2}^{(N-1)/2} h(nT)x(mT-nT) , \quad (7)$$

where T is sampling period, and $h(nT)$ is impulse response containing N non-zero coefficients.

However, implementing inversion of (1) by FIR filters for real – noisy, finite length (truncated), discretely sampled datasets often gives disappointing results manifesting as inaccurate and bursty inverted (deconvolved) waveforms, whose application for physically relevant and sensible solutions may be quite ambiguous.

The presented paper is devoted to improving the performance of FIR deconvolution filters for inversion of convolution transforms in order to attain deconvolved waveforms as accurate as possible with controllable noise amplification of the filter for a user's available input data.

To achieve this objective, first, the digital filter will be adapted to available input data. Because design of a filter producing deconvolved waveforms as accurate as possible is *data dependent problem*, adaption of the filter to the available input data promises some potentialities for the performance improvement. Second, noise amplification of the filter will be controlled in a manner minimally disturbing the frequency response by implementing natural regularization based on choosing optimal sampling rate.

The rest of the work is organized in five sections. Section 2 establishes the performance measures for FIR deconvolution filters relating to accuracy of deconvolved waveforms and noise amplification. The factors affecting the performance, such as support size, sampling rate, design methods and specifications, regularization measures, etc. are reviewed in Section 3. In Section 4, the proposed approach is described for designing FIR deconvolution filters with the desired noise gains producing maximum accurate waveforms for the predefined filter supports. Two illustrative examples of designing a digital differentiator for the logarithmic derivative [6] and a digital estimator of the distributions of relaxation times [7,8] are presented in Section 5. Here, the performance of the designed systems is compared with that of FIR filters constructed by some other commonly used techniques. Section 6 contains conclusions.

Part of the results presented herein was originally reported in the conference [9].

2. Performance of Deconvolution Filters

Traditionally, the performance of frequency-selective FIR filters, such as lowpass, bandpass, highpass filters, etc. [10], intended for removing some unwanted frequency parts or extracting some useful parts of a signal, is defined in terms of the deviation (i.e. the error) between some desired frequency response and that achieved by the designed filter. This performance measure is unrelated to data to be processed and depends mainly on the filter length (i.e. the number of filter coefficients N). In general, the longer length is, the higher is the performance.

Due to the unlike objective posed here – to produce deconvolved waveforms as accurate as possible with controllable noise amplification, the deviation between the desired frequency response and that of the digital filter is insufficient and two performance aspects – *deconvolution accuracy* and *noise amplification* shall be controlled.

2.1 Deconvolution accuracy

We propose to define *deconvolution accuracy* through the accuracy of the deconvolved waveforms likewise

to the measurement and test accuracy in the metrological documents [11-13] as: "*closeness of agreement between a sequence of deconvolved waveform and the sequence of true waveform*". The theoretical waveform $y(t)$ established by Eq. (1) or (4) will be used as true one for the definite reference signal $x(t)$. A deconvolution is said to be more accurate when it offers a smaller *deconvolution error*, which will be expressed as mean squared error between filter output $\hat{y}(mT)$ and true output $y(mT)$ for definite noiseless reference signal

$$E = (1/K)\sum_{m=1}^{K}\left[\hat{y}(mT) - y(mT)\right]^2, \quad (8)$$

where K is length of a deconvolved waveform.

2.2 Influence of Noise

Noise effect of deconvolution filter can be characterized by various imprecision measures of the deconvolved waveforms, such as SNR (signal-to-noise ratio), standard deviation, variance, etc. In this study, however, following the suggestion in [14-16], noise influence will be quantified in terms of *noise gains* showing how the noise variance σ_x^2 of signal to be processed is transmitted to the noise variance σ_y^2 of deconvolved signal

$$S = \sigma_y^2 / \sigma_x^2 .$$

The advantage of such choice is a possibility to quantify ill-posed nature of both a deconvolution problem and a deconvolution filter. Thus, the degree of ill-posedness of the deconvolution problem will be calculated by the theoretical noise gain determined by the Parseval's relation [5,10] from the ideal frequency response

$$S_{theor} = T/(2\pi)\int_{-\pi/T}^{\pi/T}\left|H(j\omega)\right|^2 d\omega, \quad (9)$$

whereas the degree of ill-conditioness of deconvolution filter will be measured by the experimental noise gain calculated through the filter coefficients

$$S_{\exp} = \sum_n h^2(nT). \quad (10)$$

Noise gains $S >> 1$ are responsible of the ill-posedness of a deconvolution problem and the ill-conditioness of the algorithms designed. Thus, noise amplification, as a rule, is not a problem for the conventional frequency-selective (lowpass, bandpass, highpass, etc.) filters [10], because condition $\left|H(j\omega)\right| \le 1$ is typically fulfilled resulting in $S \le 1$ according to the Parseval's relation. Contrary to this, square integration (9) of increasing magnitude response (6) over frequency band

$$\Omega = [-\pi/T, \pi/T] \quad (11)$$

extending when T decreases, results that $S_{theor} \to \infty$ when $T \to 0$.

The Parseval's relation shows that noise amplification or more generally the degree of ill-posedness and ill-conditioness depends on the sampling rate. Two noise gains S_{theor} and S_{exp} give simple means to ascertain whether the observed noise effect is an essential feature of the theoretical structure of a deconvolution process or it comes purely from a discrete-time algorithm used.

Above noise characterization is valid for white noise [10]. For coloured noises, the characterization should be appropriately modified.

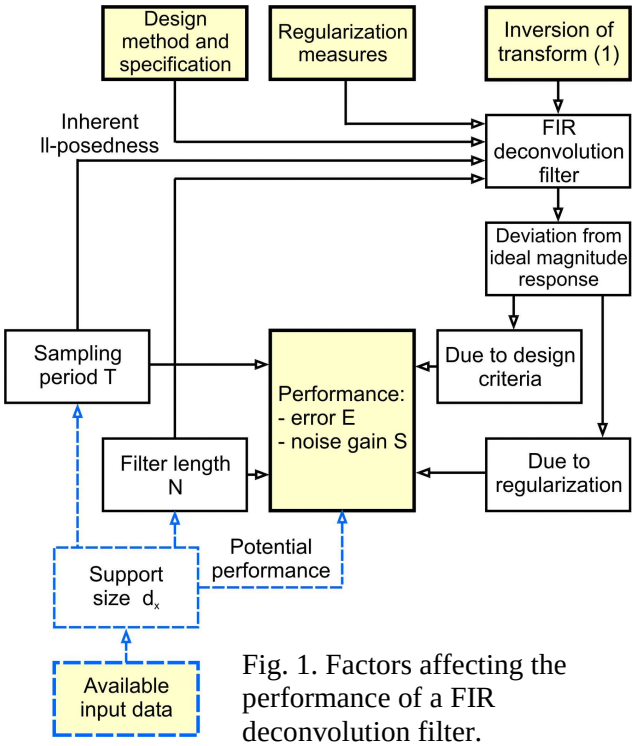

Fig. 1. Factors affecting the performance of a FIR deconvolution filter.

3 Factors Affecting the Performance

There are numerous factors affecting the performance of a deconvolution filter in rather complex and conflicting manner, between which an optimal trade-off has to be attained. In pure filtering sense, the performance of a FIR deconvolution filter depends on the filter length N and sampling period T

(Fig. 1), and is determined by the design specification defined, the design method used to find the filter coefficients, as well as the regularization measures exploited to minimize noise amplification. However, to solve a particular deconvolution problem, the filter shall be compatible with the available input data, which limits free choice of N and T. To gain a deeper understanding, the effect of some factors on the performance will be analysed below.

3.1. Support Size

Continuous support size of a deconvolution filter is equal to the length of sliding window

$$d_x = t_+ - t_- = T(N-1), \quad (12)$$

with which the filter slides over the input data sequence. Thus, d_x shall be shorter the time interval of available input sequence

$$D_x = T(M-1), \quad (13)$$

where M is number of samples of input sequence.

Physically, d_x limits information accessible for computing an output sample, and so determines the potential performance of a deconvolution filter. Thus, the support size should be long enough that N samples within it to contain information needed to calculate an output sample with the desired accuracy and noise amplification. Replacement of the infinite support size of (4) by finite one (12) is one of main reasons why the perfect deconvolution cannot be achieved by FIR filters.

In the filtering context, support size (12) affects the performance through the filter length N and sampling period T. For fixed d_x, it defines possible combinations of N and T. The larger support size promises potentially the higher accuracy of the deconvolved waveforms and the smaller noise gains, on the other hand, the larger support size, the shorter is *usable output sequence* [16] due to transient responses when the first (input-on transient) and last (input-off transient) output samples are computed from incomplete information containing zeros. After discarding these first and last output samples, a usable steady-state output sequence is obtained, which is by $N-1$ samples shorter than the input sequence. In the limit case, when the support size is equal to the input data interval, i.e. $d_x = D_x$ or $N = M$, only one usable output sample can be obtained.

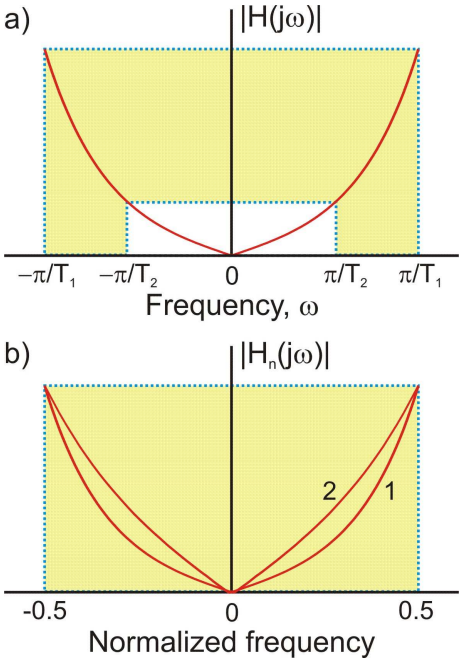

Fig. 2. Portions of infinitely increasing ideal magnitude response corresponding to two sampling periods $T_1 < T_2$ (a) and their normalized versions (b).

3.2 Sampling Rate

Despite that a general recommendation [10] suggests to choose sampling rate according to the sampling (Shannon) theorem, the answer to the question how to choose the correct sampling rate for a deconvolution filter is not as obvious as it seems at first sight because sampling affects on the performance through: (i) the signal to be processed as well as (ii) the filter to be designed.

Sampling converts continuous signal $x(t)$ into its discrete-time version and loss of information between input samples is another reason, why digital filters cannot carry out the perfect deconvolution. Thus, for band-unlimited signals considered here, some violation of the sampling theorem is unavoidable in any case. If even the correct sampling rate according to the sampling theorem can be defined for $x(t)$, this means only that $x(t)$ can be perfectly reconstructed from the discrete samples. However, the correct sampling rate for $x(t)$ does not guarantee the correct sampling rate for deconvolution result [17] because signal $y(t)$ that we wish to recover as one, from which the effect of primary convolution (1) is removed, by definition, has the broader spectrum than that of $x(t)$.

For the digital filter, sampling limits (cuts) a portion of the infinitely increasing ideal magnitude response to be approximated within frequency band

(11) (Fig. 2). This band according to the Parseval's relation (9) establishes the inherent degree of ill-posedness, which, of course, will be transformed into the actual noise amplification due to the deviations caused by non-ideal fitting.

3.3 Design Specifications and Methods

Design techniques influence the performance through: (i) design specification and criteria defined, and (ii) methods used to calculate filter coefficients [10], such as window method, frequency sampling method, weighted least squares design, minimax design, etc.

Since a filter must be adapted to the intended application, the design specification of a deconvolution filter should be defined in the way to produce deconvolved waveforms as accurately as possible. Unfortunately, such specification cannot be formulated because it is not known, how the frequency response of a digital filter to be designed shall deviate from infinitely increasing ideal one to produce accurate waveforms, and this specification depends on the data to be processed. Commonly used practice to consider a deconvolution filter as highpass one and detailing its magnitude responses into pass-, stop- and transition bands [10] can be rather subjective and can limit the potential deconvolution accuracy already in the filter specification stage.

In general, it is impossible to normalize different portions of ideal frequency response to be approximated by the digital filter at different sampling rates (see Fig. 2) to the response that is independent of the sampling rate. For example, the normalized portions in Fig. 2(b) differ from each other and can be interpreted as ones belonging to different filters. As a consequence, a deconvolution filter cannot be designed independently of the sampling rate and the filter (impulse response) obtained at one sampling rate, cannot be applied to other sampling rate. An exception is differentiators (see Sub-section 5.1), whose linearly increasing magnitude responses [10,18] allow normalization to the unity response and, so, designing differentiators in a sampling-rate invariant manner.

Due to increasing magnitude responses (6), to attain maximum accuracy, it is desirable to design linear phase deconvolution filters as type I (odd N) or type IV (even N) systems [10], which, contrary to type II and III systems, have not a restriction that their magnitude responses must be zero at end frequencies $\omega = \pm\pi / T$.

3.4 Regularization

Ill-posed nature of the inversion requires that special regularization measures [1,19,20] are used to minimize noise amplification. Despite relatively large variety and complexity of the regularization methods, they, in one way or another, decrease the areas under increasing magnitude responses, usually by suppressing the responses at higher frequencies, which according to the Parseval's relation (9) reduces the noise gains. For example, such popular techniques as Wiener filtering and Tikhonov regularization can be interpreted as a cascade of the inverse filter with frequency response (5) and some lowpass filter. From the viewpoint of the performance, such lowpass filtering represents actually the forced distortion of the frequency responses affecting, without doubt, deconvolution accuracy unfavourably.

4 Proposed Design Approach

To summarize factors affecting the performance of deconvolution filters, a conclusion can be made that the following difficulties hamper to attain deconvolved waveforms as accurately as possible:

(1) designing of accurate deconvolution filters is a data-dependent problem,
(2) it is not known how the magnitude response of a digital filter to be designed shall deviate from ideal one to produce accurate deconvolved waveforms,
(3) there are not unambiguous criteria for choosing the optimal sampling rate because: (i) formally, the unknown signal to be found in deconvolution process has a broader spectrum than that to be processed, (ii) the sampling rate, on the one hand, provokes aliasing distortions in the signal to be processed, and on the other hand, determines the inherent degree of ill-posedness of a deconvolution problem, (iii) the sampling rate together with the filter length determines the continuous support size (sliding window), which, on the one hand, restricts physically information accessible for the computing an output sample and, so, the potential performance of a deconvolution filter, and on the other hand, must be compatible to available input data,
(4) the accuracy shall be sacrificed for minimizing noise amplification due to ill-posed nature of deconvolution.

To overcome the mentioned difficulties, we propose a design approach that finds a digital filter

producing waveforms as accurate as achievable for the predefined desired noise gain S_{desired} and support size d_x. The filter is constructed in the *input-output signal domain* by learning [14-16], and S_{desired} and d_x are only design specifications. Noise amplification is controlled by varying sampling period T to alter the filter length N for the predefined d_x according to $T = d_x/(N-1)$.

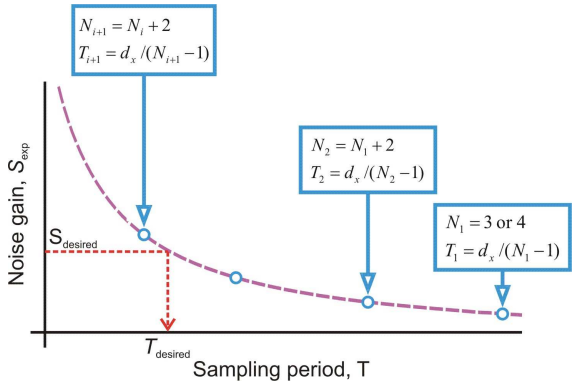

Fig. 3. Iterative process for searching an optimal combination of T and N ensuring the desired noise gain S_{desired}.

Impulse response $h(nT)$ is found for a combination of filter length N and sampling period T allowed by the predefined support size d_x, which ensures the desired noise gain S_{desired}. This combination of N and T is searched by the iterative procedure [14-16] based on typical monotonic increase of the noise gain when sampling period T decreases (Fig. 3). Trial filters are designed by learning for the combinations of T and N allowed by Eq. (12) starting at some explicitly large T_1 (e.g. corresponding to $N = 3$ or 4) yielding noise gain

$$S_{\text{exp}} < S_{desired} \tag{14}$$

by iterative increase of a number of coefficients $N_{i+1} = N_i + 2$ and the appropriate decrease of sampling period $T_{i+1} = d_x/(N_{i+1}-1)$. Once desired noise gain is reached, the iterative process is stopped and the final values of T and N are specified.

If the desired performance cannot be ensured, design specifications (S_{desired}, d_x) should be reconsidered. For example, if condition (14) cannot be achieved at the first iteration, the sampling period T_1 must be increased, which requires extension of support size d_x.

The features of the proposed approach are:

(i) Ease of design specification. Only two parameters – the desired noise gain S_{desired} and the support size (sliding window) d_x are specified.

(ii) Simplicity of regularization. The natural regularization is used based on finding minimum sampling rate, which ensures the desired noise gain. The difference between most of traditional regularization techniques [1,19,20] and the method proposed here is that the first ones minimize noise amplification at the expense of decrease of the accuracy due to distorting the frequency response at high frequencies, while the latter – the expense of decrease of the accuracy due to allowing some aliasing.

(iii) Ease of implementation. The regularized algorithm is the original discrete convolution algorithm (7) with the specified T and N.

(iv) Economical solution. The approach finds the most economical solution in the sense as one with minimum N.

(v) Optimal magnitude responses. Optimal flat (ripple-free) magnitude responses around zero frequency are obtained, which produce output waveforms as accurate as possible.

5 Illustrative Examples

The developed approach has been approbated to design FIR filters for a wide variety of interconversions between monotonic material functions [16]. Design by learning has been also used to construct FIR Kramers-Kronig transformers [21] and FIR filters for spectrum analysis and synthesis [22]. Here, as illustrative examples, designs of a differentiator for the logarithmic derivative [6] and an estimator of distribution of relaxation times [7,8] will be demonstrated.

5.1 Differentiator for Logarithmic Derivative

Ones of the most important types of digital filters are digital differentiators [18], which are widely used to calculate the change rate of recorder data. An ideal differentiator has pure imaginary frequency response $H(j\omega) = j\omega$ [10] resulting in linearly increasing magnitude response, which, in its turn, causes inversely proportional dependence of the impulse response to sampling period

$$h(nT) = h(n)/T, \tag{15}$$

where $h(n)$ is the impulse response normalized to unity sampling rate.

In literature, differentiators usually are not treated as deconvolution filters, although differentiation is a

typical deconvolution operation averting integration, i.e. inverting convolution transform with kernel $k(t)$ in form of a step function. An ideal differentiator satisfies condition (6) and according to the Parseval's relation (9) has theoretical noise gain

$$S_{theor} = \pi^2 / 3T^2 . \quad (16)$$

FIR digital differentiators have been the subject of numerous investigations [18]. A variety of methods with different design criteria, such as the Remez exchange algorithm [23], the window method [10], the weighted least squares method [24,25], Taylor series [26], maximal linearity constraints [27], hybrid optimization method [28], etc. have been developed. This is by no means the exhaustive list. Such vast variety of the methods confirms the fact that there is no unique solution for a "universal" digital differentiator, as well as – for a "universal" deconvolution filter in general, and design of deconvolution filters is data-dependent problem.

For dielectrics, the logarithmic derivative of the real part of complex dielectric permittivity $\varepsilon'(\omega)$ [6]

$$\varepsilon''_D(\omega) = \partial\varepsilon'(\omega) / \partial \ln\omega \quad (17)$$

is used for estimation of the imaginary part $\varepsilon''(\omega)$. By denoting $y(\omega) = \varepsilon''_D(\omega)$ and $x(\omega) = \varepsilon'(\omega)$ and introducing substitution $t = \ln\omega$, Eq. (17) may be rewritten as:

$$y(e^t) = \partial x(e^t) / \partial t . \quad (18)$$

Suppose that a user wants to construct a differentiator with the desired noise gain

$$S_{desired} \approx 10 \quad (19)$$

producing maximum accurate waveforms for the logarithmic derivative (17) to employ, for example, support size $d_x = 1$.

To attain maximum accuracy, the differentiator shall be designed as type IV filter [10] with an even number of coefficients. So, to choose a minimum number of coefficients $N = 4$, from Eq. (12) it follows

$$T_1 = d_x / (N - 1) = 0.333 .$$

Design of the differentiator by learning, using the following training functions:

$$x(t) = 1/(1+t^2),\ y(t) = -2t/(1+t^2)^2 ,$$

gave the normalized coefficients listed in Table 1. According to Eq. (10), they provide the noise gain $S_{\exp} = 23.22$ exceeding the desired value (19). In line with the proposed procedure (see Section 4), support size d_x should be extended and increased sampling period T_1 should be used.

Table 1. Coefficients of the differentiator designed by learning

$h(-1/2) = -h(1/2)$	1.1349626
$h(-3/2) = -h(3/2)$	-0.045064591

However, due to normalization (15), differentiators may be constructed in the sampling-rate invariant manner, and $T_{desired}$ can be found by an expression

$$T_{desired} = T\sqrt{S_{\exp} / S_{desired}} = 0.33\sqrt{23.22/10} = 0.51$$

coming from simple mathematical manipulations of Eqs. (10) and (15). Thus, the designed 4-point differentiator ensures the desired noise gain (19) at $T_{desired} = 0.51$ and requires support size $d_x = 1.53$. Due to non-ideal fitting, T_{desired} differs from the sampling period coming from theoretical noise gain (16)

$$T_{theor\,S=10} = \pi\sqrt{1/3/S_{desired}} = 0.57 .$$

The designed differentiator was compared with 4-point linear phase differentiators designed by the Remez exchange algorithm [23] and by using maximally linearity constraints [26,27]. The coefficients of these filters are given In Table 2, while the normalized magnitude responses are shown in Fig. 4.

Table 2. Coefficients of the equiriple minimax and maximally linear differentiators

	Equiriple minimax	Maximally linear
$h(-1/2) = -h(1/2)$	1.3091930	1.1249996
$h(-3/2) = -h(3/2)$	-0.13106367	-0.041666936

The differentiators have been tested for $\varepsilon'(\omega)$ corresponding to single Debye relaxation [16]

$$x(e^t) = \frac{1}{1+e^{2t}} \quad (20)$$

representing the worst case in signal processing sense with maximum wide spectrum. Function (20) has the derivative:

$$y_{exact}(e^t) = \frac{2t^2 e^{2t}}{(1+e^{2t})^2}. \quad (21)$$

In Fig. 5, error curves of $\Delta y = \left|\hat{y}(e^t) - y(e^t)\right|$ are shown for the three differentiators operating at $T = 0.5$ and $T = 0.7$, whereas the performance parameters are summarized in Table 3. As it is seen, the differentiator designed here has the highest accuracy, although its performance is very close to that of the maximally linear differentiator. So, maximally flat differentiators should be used as the next more favourable option. Contrary, the equiriple minimax differentiator produces noticeably inaccurate waveforms and obviously is not suitable for the logarithmic derivative.

5.2 Estimator of Distribution of Relaxation Times

As it is known [7,8], the distribution of relaxation times (DRT) – a quantity coming also from the material science [16], is an attribute of the response functions of systems (materials), whose time-domain behaviour does not comply with the simple exponential law. It is generally accepted that the impulse responses of such systems result from the superposition of exponential processes with certain relaxation times forming the appropriate non-negative DRT functions. DRT recovery is categorized as one of all the time the most challenging and hard ill-posed inversion problems.

Here, we consider DRT recovery from the real part of complex dielectric permittivity $\varepsilon'(\omega)$ – the same function has been used for calculating the logarithmic derivative in the previous Sub-section, which requires inversion of an integral transform [7,8]

$$\varepsilon'(\omega) = \int_0^\infty \frac{y(\tau)}{1+\omega^2\tau^2}\frac{d\tau}{\tau}, \quad 0 < \omega < \infty, \quad (22)$$

where τ is relaxation time, and $y(\tau)$ is the function of DRT. For $x(\omega) = \varepsilon'(\omega)$ and substitutions

$$t = \ln\omega \text{ and } u = -\ln\tau, \quad (23)$$

Eq. (22) can be converted into the following convolution transform

$$x(e^t) = \int_{-\infty}^{\infty} \frac{y(e^{-u})}{1+e^{2(t-u)}}du. \quad (24)$$

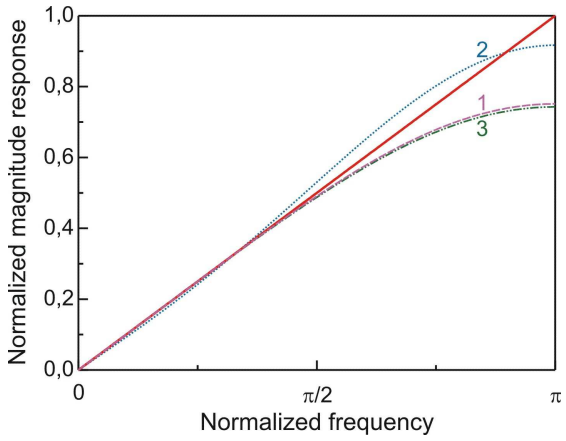

Fig. 4. Normalized magnitude responses of 4-point digital differentiators: 1 – designed by learning, 2 – equiriple minimax, 3 – maximally linear.

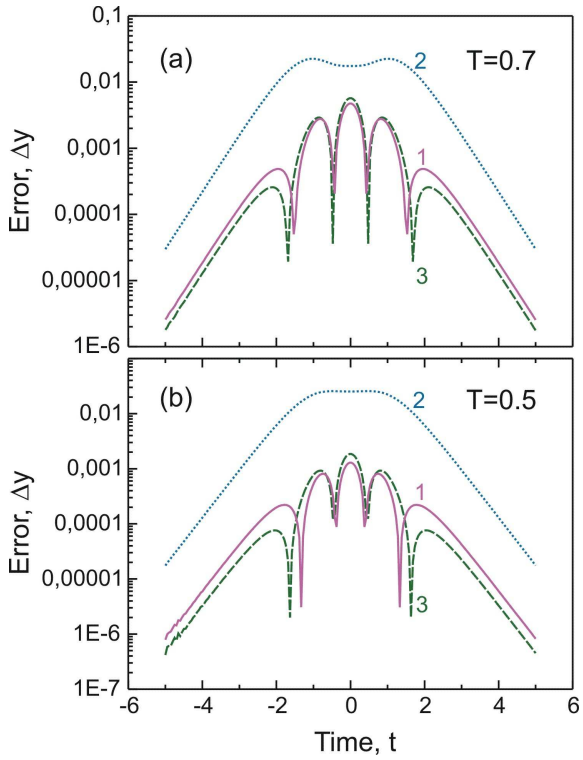

Fig. 5. Error curves for deconvolved waveform (21) produced by 4-point differentiators: 1 – designed by learning, 2 – equiriple minimax, 3 – maximally linear.

The inverse kernel for transform (24) exists in the class of the generalized functions. To the best of our knowledge, its analytic expression is not known at present, however, according to (5) one can derive its Fourier transform representing the frequency

response of ideal DRT estimator [7,8]

$$H(j\omega) = j(2/\pi)\mathrm{sh}(\pi\omega/2)\,. \qquad (25)$$

Table 3. Performance parameters

T	0.5	0.7
S_{theor}	13.16	6.71
Differentiator designed by learning		
E	$0.254\cdot 10^{-4}$	0.00429
S_{exp}	10.32	5.37
Equiriple minimax differentiator		
E	0.0337	0.0256
S_{exp}	13.9	7,29
Maximally linear differentiator		
E	$0.459\cdot 10^{-4}$	0.00495
S_{exp}	10.14	5.28

The magnitude response for (25) (Fig. 6) is an extremely fast growing function (pay attention on logarithmic scale of Y axis) pointing on a high degree of the ill-posedness of DRT recovery problem.

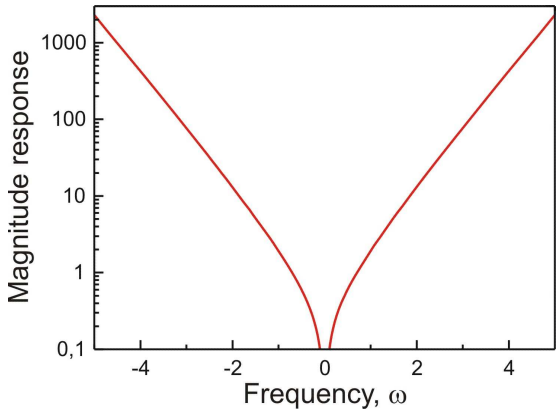

Fig. 6. Magnitude response of ideal DRT estimator.

As an illustrative example, consider design of a digital DRT estimator with the desired noise gain (19) employing support size $d_x = 6$. Similarly to differentiators, DRT estimators shall be designed as linear phase systems of type IV [10] to attain maximum accuracy. The magnitude responses of DRT estimators cannot be normalized to unity sampling rate, so, the estimators have to be designed at the specified sampling rates.

According to Eq. (12), minimum filter length $N = 4$ with sampling period $T_1 = 2$ shall be used in the first iteration, while $N_2 = 6$ and $N_3 = 8$ with $T_2 = 1.2$ and $T_3 = 0.857$ respectively must be chosen at the second and third iterations. The estimators were designed by using the training functions corresponding to Cole-Cole relaxation model [29]. In Fig. 7(a), the magnitude responses are shown for the filters obtained in the first three iterations with the highlighted areas under the responses, whereas in Fig. 7(b) variation of noise gain S_{exp} and error E is presented as functions of the sampling period.

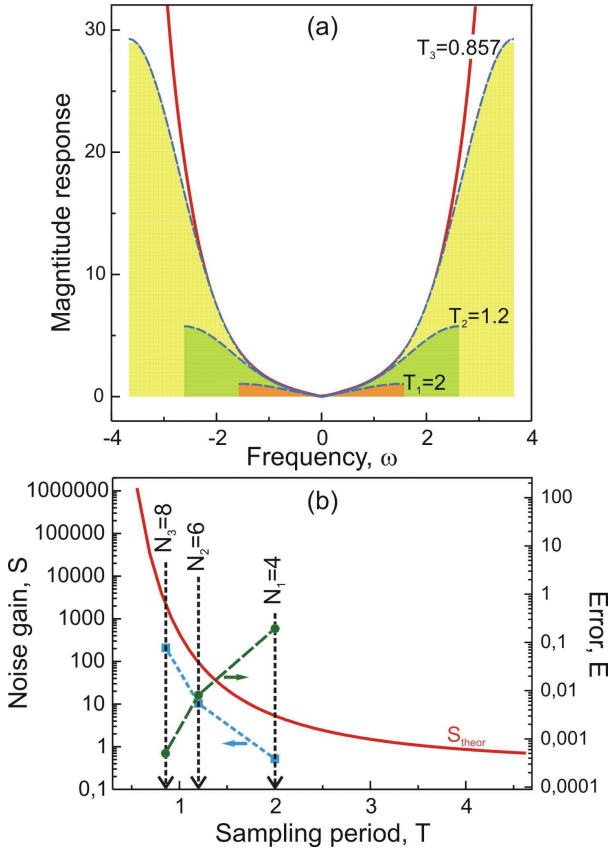

Fig. 7. Magnitude responses (a) and variation of the noise gain and the error (b) of trial filters in the first three iterations. Shaded regions in (a) show the areas under the magnitude responses; the solid line in (a) is the ideal magnitude response. The solid line in (b) shows the theoretical noise gain.

As it is seen, the magnitude responses are ripple-free (flat) coinciding very accurately with the ideal one in a region of approximately $(0.3-0.6)\Omega$ centred at zero frequency. The areas under the magnitude responses increase significantly with decreasing the sampling period causing great augment in the noise gain. Due to the non-ideal fitting, the experimental noise gain is smaller than the theoretical one. The augment in the noise gain, however, is accompanied by favourable effect of approximately the same decrease in the error. It is interesting to note that the error E decreases approximately inversely proportionally to the noise gain S in accordance with the relationship $E \approx 0.1/S$.

The 6-point filter obtained in the second iteration has noise gain $S_{\exp} = 10.35$ satisfying condition (19), so, it could be taken as the maximum accurate estimator for $d_x = 6$. The coefficients of this filter are given in Table 4.

Table 4. Coefficients of 6-point DRT estimator

$h(-1/2) = -h(1/2)$	-2.25364
$h(-3/2) = -h(3/2)$	0.577504
$h(-5/2) = -h(5/2)$	-0.0621334

Experiments have been carried out for designing DRT estimators also by the frequency sampling method [10]. However, they showed that the frequency sampling method does not allow obtaining really working DRT estimators for the reason that the method cannot provide sufficiently good fit of the fast growing magnitude responses for the support sizes usable in practice.

Fig. 8 shows the magnitude responses of 8-point estimators designed by the frequency sampling method and by learning (this is the filter obtained at the third iteration above). Contrary to the learning method, the frequency sampling method generates a filter with large ripples resulting in the deconvolved waveforms, which have little in common with the true solutions. At the same time, noise gain of the filter is approximately 7 greater to compare with the estimator designed by learning.

A conclusion can be made that 8 coefficients are insufficient for the frequency sampling method to provide sufficiently good fit. Unfortunately, there is no way out of the situation for the fixed support size. Increase of a number of filter coefficients N decreases sampling period T, which according to (11) expands band Ω and so the portion of the fast growing ideal magnitude response to be approximated by the digital filter.

The fitting quality may be improved by approximating the smaller portion of the fast growing ideal magnitude response with the larger number of coefficients, which requires increasing sampling period T and extending support size d_x. For example, at $T = 1.67$ (which limits the noise amplification to the level $S_{theor} < 10$) and $N = 16$ requiring the support size

$$d_x = 25.05, \tag{26}$$

the frequency sampling method generates an estimator with magnitude response 1 shown in Fig. 9. However, despite the relatively good fit and acceptably low noise amplification, the estimator does not work well. In Fig. 10, the waveforms are compared for an asymmetric DRT obtained by 16-point estimators designed by the frequency sampling method (waveform 1) and learning (waveform 2). In contrast to excellently deconvolved waveform 2, waveform 1 is biased and contains regions with physically senseless negative values at small (not shown) and large τ.

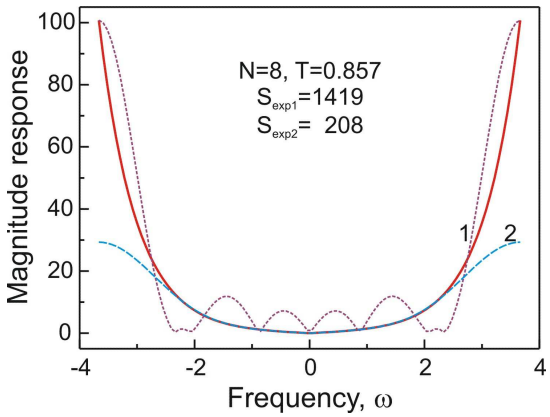

Fig. 8. The magnitude responses of 8-point estimators: 1 – designed by the frequency sampling method, 2 – designed by learning. The solid line shows the ideal magnitude response.

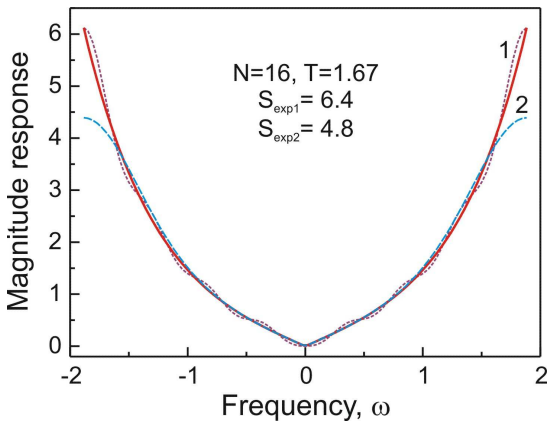

Fig. 9. The magnitude responses of 16-point estimators: 1 – designed by the frequency sampling method, 2 – designed by learning. The solid line shows the ideal magnitude response.

Unfortunately, none of these 16-point estimators is applicable in practice due to unrealistic large support size. One has to remember that the 'time domain' for DRT estimators according to (23) relates to the logarithmic frequency scale

$$d_x = t_+ - t_- = \ln \omega_+ - \ln \omega_- = \ln(\omega_+ / \omega_-)$$

resulting in

$$\omega_+ / \omega_- = \exp(d_x)$$

and transforming the support size (26) into one practically unattainable on the linear scale

$$\omega_+ / \omega_- = \exp(20.05) = 7.57 \cdot 10^{10} = 10.88 \text{ decades.}$$

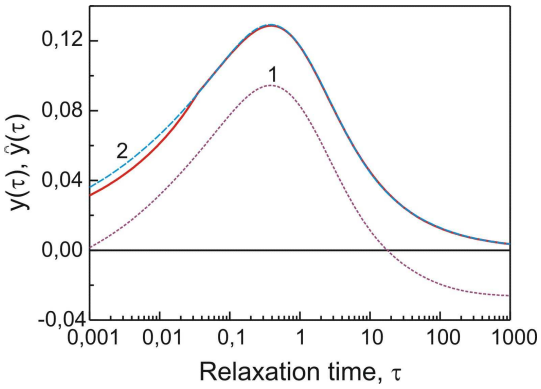

Fig. 10. DRT waveforms deconvolved by 16-point estimators: 1 – designed by the frequency sampling method, 2 – designed by learning. The solid line shows the true waveform.

6 Conclusions

Inversion of convolution transforms by FIR deconvolution filters has been considered from the perspective attaining deconvolved waveforms with the highest possible accuracy for user's predefined noise gains and filter supports. The following difficulties have been disclosed hampering to gain this goal:

(1) designing maximum accurate deconvolution filters is a data-dependent problem,
(2) it is not known how the magnitude response of a filter to be designed shall deviate from ideal one to produce deconvolved waveforms as accurate as possible,
(3) there are not unambiguous criteria for choosing the optimal sampling rate because: (i) formally, the unknown signal to be found by the inversion has a broader spectrum than that to be processed, (ii) the sampling rate, on the one hand, provokes aliasing distortions in the signal to be processed, and on the other hand, determines the inherent degree of ill-posedness of a deconvolution problem, (iii) the sampling rate and the filter length determines the support size, which, on the one hand, restricts physically information accessible for the computing an output sample and, so, the potential performance of a deconvolution filter, and on the other hand, must be compatible to available input data,
(4) the accuracy shall be sacrificed for minimizing noise amplification due to ill-posed nature of the inversion.

To overcome the mentioned difficulties, a design approach has been developed based on learning in input-output signal domain and controlling noise amplification by varying sampling rate, which allows generating maximum accurate FIR filters for the prescribed noise gains and support sizes.

As examples, designs of a digital differentiator for the logarithmic derivative and an estimator of the distributions of relaxation times (DRT) have been demonstrated by the developed approach. It has been found that a common feature of the filters producing accurate waveforms is flat (ripple-free) magnitude responses around zero frequency. The differentiator designed by the proposed approach demonstrates the higher accuracy and the lower noise gain over the filter constructed by the Remez exchange algorithm, however, gives approximately the same performance as the maximally linear differentiator. It has been ascertained that the frequency sampling method does not allow obtaining really working DRT estimators due to inability to ensure sufficiently good fit of the fast growing magnitude responses for the support intervals accessible in practice.

Acknowledgements

This work was supported by the European Regional Development Fund (ERDF) under project No. 2010/0213/2DP/2.1.1.1.0/10/APIA/VIAA/017.

References:

[1] P.C. Hansen, *Rank-Deficient and Discrete Ill-Posed Problems. Numerical Aspects of Linear Inversion*, SIAM, 1998.
[2] E.M. Lifshitz, L.D. Landau, *A Shorter Course of Theoretical Physics*: Vol. 1: Mechanics and Electrodynamics, Pergamon Press, 1972.
[3] J.D. Ferry, *Viscoelastic Properties of Polymers*, 3rd. ed., J. Wiley and Sons, 1980.
[4] N.G. McCrum, B.E. Read, G. Wiliams, *Anelastic and Dielectric Effects in Polymer Solids*, J. Wiley and Sons, 1967.
[5] A. Korn, T. M. Korn, *Mathematical Handbook for Scientists and Engineers*, second, enlarged and revised ed., McGraw-Hill Book Company, 1968.

[6] H. Haspel, Á. Kukovecz, Z. Kónya, I. Kiricsi, Numerical Differentiation Methods for the Logarithmic Derivative Technique Used in Dielectric Spectroscopy, *Processing and Application of Ceramics*, Vol. 4, No. 2, 2010, pp. 87–93.

[7] V. Shtrauss, Determination of Relaxation and Retardation Spectrum by Inverse Functional Filtering, *J. Non-Newtonian Fluid Mech*., Vol. 165, 2010, pp. 453-465.

[8] V. Shtrauss, Determination of the Relaxation and Retardation Spectra – a View from the Up-To-Date Signal Processing Perspective, *Mechanics of Composite Materials*, Vol. 48, No. 1, 2012, pp. 27-46.

[9] V. Shtrauss, A User-Oriented Approach to Designing FIR Deconvolution filters, in: *Proc. 12th WSEAS International Conference on Systems Theory and Scientific Computation, Advances in Systems Theory, Signal Processing and Computational Science*, Istanbul, Turkey, August 2012, pp. 130-135.

[10] A.V. Oppenheim, R.V. Schafer, *Discrete-Time Signal Processing*, Sec. Ed., Prentice-Hall International, 1999.

[11] JCGM 200:2012, *International Vocabulary of Metrology – Basic and General Concepts and Associated Terms* (VIM), 3rd edition, (JCGM 200:2008 with minor corrections).

[12] ISO 5725-1:1994. *Accuracy (Trueness and Precision) of Measurement Methods and Results – Part 1: General Principles and Definitions*.

[13] ANSI/ISO/ASQ 3534-1:2006: *Statistics – Vocabulary and Symbols – Part 1: General Statistical Terms and Terms Used in Probability*.

[14] V. Shtrauss, Decomposition of Multi-Exponential and Related Signals – Functional Filtering Approach, *WSEAS Trans. Signal Processing*, Vol. 4, Issue. 2, 2008, pp. 44-52.

[15] V. Shtrauss, Sampling and Algorithm Design for Relaxation Data Conversion, *WSEAS Trans. Signal Processing*, Vol. 2, Issue 7, 2006, pp. 984-990.

[16] V. Shtrauss, Digital Interconversion between Linear Rheologic and Viscoelastic Material Functions. In: *Advances in Engineering Research*. Vol. 3, Ed. V.M. Petrova, Nova Science Publishers, 2012, pp. 91-170.

[17] P. Magain, F. Courbin, S. Sohy, Deconvolution with Correct Sampling, *Astrophysical Journal*, No. 1, 1998, pp. 472-477.

[18] S.C. Dutta Roy, B. Kumar, Digital Differentiators. In: *Handbook of Statistics*, Vol. 10, Eds. N.K. Bose, C.R. Rao, Elsevier, 1993, pp. 159–205.

[19] M. Iqbal, Deconvolution and Regularization for Numerical Solutions of Incorrectly Posed Problems, *J. Comput. Appl. Math*., Vol. 151, 2003, pp. 463–476.

[20] H.W. Engl, M. Hanke, A. Neubauer, *Regularization of Inverse Problems*, Kluwer, 1996.

[21] V. Shtrauss, FIR Kramers-Kronig Transformers for Relaxation Data Conversion, *Signal Processing*, Vol. 86, 2006, pp. 2887-2900.

[22] V. Shtrauss, Spectrum Analysis and Synthesis of Relaxation Signals, *Signal Processing*, Vol. 63, 1997, pp. 107-119.

[23] T.W. Parks, J.H. McClellan, Chebyshev Approximation for Nonrecursive Digital Filters with Linear Phase, *IEEE Trans. Circuit Theory*, Vol. 19, 1972, pp. 189–194.

[24] S. Sunder, W.S. Lu, A. Antoniou, Y. Su, Design of Digital Differentiators Satisfying Prescribed Specifications Using Optimization Techniques, *IEE Proc.*, Vol. 138 G, 1991, pp. 315-320.

[25] S. Sunder, V. Ramachandran, Design of Equiripple Nonrecursive Digital Differentiators and Hilbert Transformers Using a Weighted Least-Squares Technique, *IEEE Trans. Signal Process.*, Vol. 42, No. 9, 1994, pp. 2504-2509.

[26] I.R. Khan, R. Ohba, New Design of Full Band Differentiators Based on Taylor Series, *IEE Proc. – Vis. Image Signal Process.*, Vol. 146, No.4, 1999, pp. 185–189.

[27] I.R. Khan, M. Okuda, R. Ohba, Design of FIR Digital Differentiators Using Maximal Linearity Constraints, *IEICE Trans. Fundamentals*, Vol. 87-A, No. 8, 2004, pp. 2010-2017.

[28] D. Singh, R. Kaur, Hybrid Optimization Technique for the Design of Digital Differentiator, *Recent Researches in Circuits, Systems, Mechanics and Transportation Systems*, 2011, pp. 52-57. http://www.wseas.us/e-library/conferences/2011/Montreux/MECHICSE/MECHICSE-08.pdf.

[29] K.S. Cole, R.H. Cole, Dispersion and Absorption in Dielectric. Alternating Current Characteristics, *J. Chem. Phys.*, Vol. 9, 1941, pp. 341-351.